Theoretical and experimental study of energy loss of Li ions in Zn

C. C. Montanari* and J. E. Miraglia
Instituto de Astronomía y Física del Espacio and Departamento de Física, Facultad de Ciencias Exactas y Naturales, Universidad de Buenos Aires, Buenos Aires, Argentina

M. Behar and P. F. Duarte
Instituto de Física, Universidade Federal do Rio Grande do Sul, Avenida Bento Goncalves 9500, 91501-970, Porto Alegre, RS, Brazil

N. R. Arista, J. C. Eckardt, and G. H. Lantschner
Centro Atómico Bariloche, Comisión Nacional de Energía Atómica, 8400 S. C. de Bariloche, Argentina
(Received 27 July 2007; revised manuscript received 25 February 2008; published 4 April 2008)

We have performed a combined theoretical and experimental study of the energy loss of Li ions in Zn, on a wide range of energies, together with comparative studies for H and He ions on the same target. By using Zn films and the Rutherford backscattering technique, we were able to determine the stopping power for Li ions in the (0.3 to 5) MeV energy interval. The experimental results cover an energy range which includes the maximum of the stopping power. The values obtained agree well with previous measurements performed in a limited energy interval and with the semiempirical code SRIM 2006. On the other hand, we have performed *ab initio* theoretical calculations based on the extended Friedel sum rule–transport cross section formulation for the valence electrons and the shellwise local plasma approximation for the inner shells. This theoretical description reproduces reasonably well the experimental results on the whole studied energy range. The same occurs with previous measurements performed with H and He on the same target. The importance of the screened potential on the stopping power due to the valence electrons is stressed in the present description.

DOI: 10.1103/PhysRevA.77.042901 PACS number(s): 34.50.Bw

I. INTRODUCTION

Despite the technological uses of zinc and the applications of the stopping power data to material science, measurements of stopping power of Zn for different ions are scarce in comparison with other solids (see, for instance, the tabulations by Ziegler [1] or Paul [2], and references therein). This scarcity of data is mainly due to difficulties in the preparation of thin zinc samples by evaporation due to its condensation properties.

To our knowledge, there are only two sets of stopping power data of Li ions in Zn available in the literature. The first one by Mertens and Krist [3] in a region around 300 keV, and the second one by Väkeväinen [4] for energies above 1.5 MeV. On the other hand, there are semiempirical predictions by the code SRIM 2006, but there is a lack of first-principle theoretical calculations that could allow systematic comparisons for the three lightest elements (hydrogen, helium, and lithium).

Therefore, we have undertaken the present work with two purposes. First, to measure the stopping power for Li in Zn on a wide energy range, in particular passing through its maximum value. And second, because its description (and comparative study for other light ions) is a challenge for the theoretical description.

The measurements were performed on Zn thin films using the Rutherford backscattering (RBS) technique at the Instituto de Física of the Universidade Federal do Rio Grande do Sul (IF-UFRGS), Brazil. The theoretical development treats separately the contributions of the valence electrons and the target inner shells. The valence electron contribution is calculated in the binary collisions framework using the extended Friedel sum rule–transport cross section (EFSR-TCS) scheme [5–7]. The core electron contribution is calculated in the approximation of an inhomogeneous free electron gas [8–13] within the shellwise local plasma approximation (SLPA) [14]. This means that the response of each shell of target electrons is calculated independently, and the threshold energy of each shell is considered explicitly by employing the Levine and Louie dielectric function [15].

II. EXPERIMENTAL PROCEDURE

The determination of stopping power of Li in Zn was done using a system of multilayer films composed by Au (5 nm)/Zn/Au (5 nm) deposited on Si wafers. These films were produced in the Centro Atómico Bariloche, Argentina. First a thin film of Au (5 nm) was evaporated on the Si wafer. This was done because the Zn atoms do not stick on Si. Then, Zn films of different thickness were deposited, and on top of each another thin Au layer (5 nm) was evaporated in order to have an additional marker. They were analyzed using proton beams with energies between 400 and 1000 keV from the 3 MV Tandetron of the IF-UFRGS, Brazil. The thickness of each Zn film was determined with these beams since the proton stopping power of Zn is well known [16,17]. To this end we have used the Rutherford backscattering technique detecting the backscattered protons with a Si barrier detector with a total resolution of 7 keV. Each film was measured several times at different geometries in order to minimize the errors. In this way, we have determined that the thickness of

*mclaudia@iafe.uba.ar

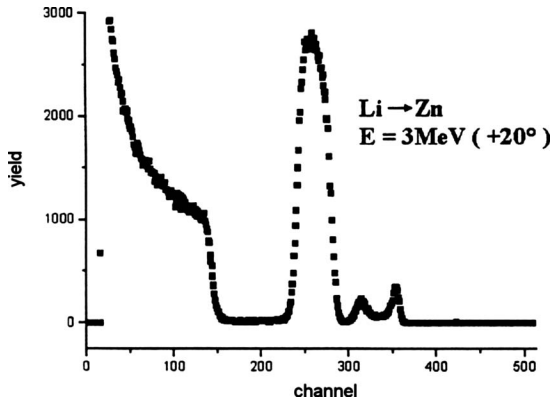

FIG. 1. ^{7}Li RBS spectrum of a Au/Zn/Au system taken at 3 MeV, with the normal of the sample at 20° with respect to the direction of the beam.

the Zn films used in the present experiments were of (46 ± 2) nm, (75 ± 3) nm, and (150 ± 5) nm, respectively. In the present case we have used the proton stopping powers quoted in Ref. [17] to obtain the above-mentioned values. The quoted errors were due to uncertainties in the energy loss determinations.

In order to determine the stopping power for Li in Zn we have used a ^{7}Li beam provided by the same accelerator. The energy range covered by the present measurements reached from 300 up to 5000 keV. The sample was mounted on a four axis goniometer. For each energy the angle between the normal to the sample and the beam was varied between 0 and 60 degrees maintaining fixed the detector position. In the present case the combined detector and electronic resolution was of the order of 15 keV. The selection of each sample was done according to the energy of the beam. In Fig. 1 we show a typical RBS spectrum of the multilayer system taken at 3 MeV with the sample inclined at 20 degrees. It can be clearly observed that the two peaks of the Au markers and the main peak corresponding to Zn are well separated.

We have used the $^{16}O(\alpha,\alpha')^{16}O$ reaction at $E = 3035$ keV or at larger energies, in order to check the O content in the samples. The obtained results indicate that the O concentration was less than 3%. In addition, in order to minimize the ion beam induced damage on the sample, for each energy we have used a fresh spot by shifting its position with the fourth axes of the goniometer.

III. DATA ANALYSIS AND EXPERIMENTAL RESULTS

We evaluated the energy loss ΔE of the Li ions in the Zn layer of thickness Δx by determining the position of the edges of the corresponding energy distribution. We note that the edges of these energy distributions appear smeared out. In the case of the front edge this is due to the experimental resolution, and in the case of the back edge the origin is a combination of the energy loss straggling and the experimental resolution (there is another, however negligible, contribution arising from the energy loss straggling in the frontal gold layer in both cases). Since the maximum energy transferred in a single process is much smaller than the above-mentioned energy loss straggling, following Bohr criterion [18], the energy loss distribution has a Gaussian shape. As the experimental resolution is also Gaussian-like, we could fit the edges with the erf fitting function (or the complementary one when dealing with the leading edge).

The stopping power dE/dx was obtained from the experimental data for Li ions backscattered at a depth x of the film, through the following relation based on the surface energy approximation [19]:

$$\Delta E(x) = \left.\frac{xK}{\cos\theta_1}\frac{dE}{dx}\right|_{E_0} + \left.\frac{x}{\cos\theta_2}\frac{dE}{dx}\right|_{KE_0}. \quad (1)$$

Here K is the kinematic factor and θ_1 and θ_2 are the angles between the sample normal with the incoming beam and the detector position, respectively, and $dE/dx|_E$ is the stopping power of Zn for Li ions of energy E. Considering Eq. (1) for ions backscattered at the back of the film, x equals the film thickness Δx, and this equation becomes an equation with two variables which can be determined when measuring at two (or more) different geometries, i.e., sets of angles θ_1 and θ_2.

This equation can be rewritten as

$$\left.\frac{dE}{dx}\right|_{KE_0} = m \left.\frac{dE}{dx}\right|_{E_0} + n, \quad (2)$$

where $m = -K(\cos\theta_2/\cos\theta_1)$ and $n = \cos\theta_2 \Delta E/\Delta x$. When measuring at two different geometries one obtains a pair of equations which can be solved obtaining the $dE/dx|_{E_0}$ and $dE/dx|_{KE_0}$ values which corresponds to the stopping powers for the energies E_0 and KE_0.

For each energy E_0 we have performed four measurements under different geometrical conditions in order to improve the precision. The stopping values were taken as the mean values of the results from the six different possible combinations of equation pairs. The errors of the present measurements were estimated to be about 5% by taking into account the dispersion and the reported uncertainties of the foil thickness determination. An additional error source are the systematic deviations due to the employed method based on surface energy approximation which leads to deviations of +5% and +2.5% at the lowest energies, 0% at the energy loss maximum, and −1% above this maximum. It should be stated that for several energies (particularly the intermediate ones) two sets of Zn films of different thickness were used and the obtained results have agreed with each other within the experimental errors. Therefore, we can conclude that the quoted results are independent of the thickness of the film used in the experiment, as expected.

Proceeding in the same way for each energy, we obtain the corresponding stopping power displayed in Fig. 2. This data are based on the proton stopping power chosen in the present case [17]. If other proton databases are used, then the present results should be renormalized. However, the comparison with previous experimental data [3,4], also included in Fig. 2, shows a quite good agreement with the present values, in particular in the high-energy region, proving that the selection of the Ref. [17] data was quite reasonable.

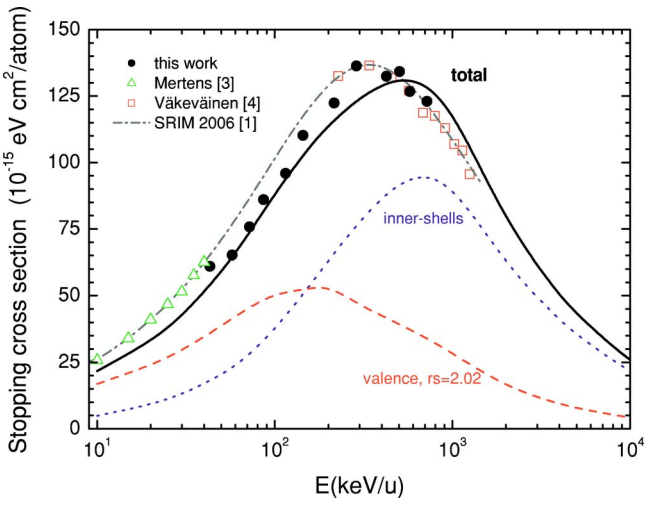

FIG. 2. (Color online) Total stopping of Li in Zn. Symbols: solid circles, this work; open triangles, Mertens *et al.* [3]; open squares, Väkeväinen [4]. Curves: solid line, our total results; dotted line, contribution of inner shells; dashed line, valence electron contribution. We also include the SRIM 2006 curve [1] in the dashed-dotted line

IV. THEORETICAL CALCULATIONS

We consider a beam of ions with atomic number Z_P moving through a medium with velocity v. The collisional processes lead to a gradual energy dissipation of the beam. In the energy range of the present calculations (10–10 000 keV/u), this energy loss is due to the inelastic stopping by the target electrons, except at the lowest energies where the elastic scattering with the atomic cores varies from 12% at 10 keV/u down to 2% at 40 keV/u to become insignificant at higher energies [1]. A good description of the nuclear stopping and possible corrections may be found in Ref. [20].

In the case of dressed ions, loss and capture processes will take place until reaching a certain equilibrium distribution of charge states q ($q=0,\ldots,Z_P$) within the foil, which depends on the impinging velocity. In this equilibrium regime, the stopping cross section S will be the sum of those S_q corresponding to each projectile with charge state q weighted with the fraction of charge $\phi_q(v)$ [21]; that is,

$$S(v) = \sum_{q=0}^{Z_P} \phi_q(v) S_q(v). \tag{3}$$

The S_q stopping cross section is determined by the interaction of the dressed ion with $N=Z_P-q$ bound electrons, and all the target electrons. In a first approximation, we will only consider the screening contribution to the stopping power (projectile electrons frozen in their ground state screening the interaction of the nucleus with the target electrons). However, target electrons interact both with the partially screened nucleus and with individual projectile electrons giving rise to a total inelastic stopping that includes ion excitation or electron loss. This contribution, which is usually denoted as antiscreening [22], was calculated for the case of He ions in Zn, being less than 1% [14]. Hence, in this paper we consider only the usual screening mode of stopping power.

The Fourier transform of the screened Coulomb potential can be expressed as

$$V(k) = -\frac{4\pi}{k^2}\rho_q(k), \tag{4}$$

with $\rho_q(k)=Z_P-\Sigma_{n=1}^{N}\langle\varphi_n|e^{i\mathbf{k}\cdot\mathbf{r}}|\varphi_n\rangle$ being an inhomogeneous effective charge of the projectile screened by the N bound electrons [23]. This $\rho_q(k)$ may be expressed analytically in terms of the Slater-type expansions for the atom. In the case of Li ions, $\rho_q(k)$ are given by

$$\rho_q(k) = 3 - N_{1s}Z_{1s}(k) - N_{2s}Z_{2s}(k), \tag{5}$$

with N_{1s} and N_{2s} being the number of electrons bound in these shells of Li^{+q}, if any. The screening functions $Z_{nl}(k)$ take simple expressions given by

$$Z_{1s}(k) = 1/[1 + X_{1s}(k)/4]^2, \tag{6a}$$

$$Z_{2s}(k) = [1 - 3X_{2s}(k) + 2X_{2s}^2(k)]/[1 + X_{2s}(k)]^4, \tag{6b}$$

with $X_{nl}(k)=k^2/(-2n^2\varepsilon_{nl})$. The binding energies, ε_{nl}, employed in this work for Li^0 and Li^+ are those by Clementi and Roetti for neutral and positive ions [24] ($\varepsilon_{1s}=-2.792\,38$ a.u. for Li^+, and $\varepsilon_{1s}=-2.460\,19$; $\varepsilon_{2s}=-0.194\,89$ a.u. for Li^0). Note that

$$\rho_q(k) = \begin{cases} Z_P & \text{when } k \to \infty \text{ (close collisions)}, \\ q & \text{when } k = 0 \text{ (distant collisions)}. \end{cases} \tag{7}$$

We shall return to this point to emphasize that for the inner shells (i.e., K and L shells of Zn), the main contribution comes from large k, so that the screening of the ion by its passive electrons is not very relevant. On the contrary, for the outer shells (M shell and the valence electrons of Zn), the main contribution comes from the region of small k and the ion charge is strongly screened.

The total stopping cross section for Li^{+q} can be expressed as

$$S_q = S_{q,\text{valence}} + \sum_{n\ell} S_{q,n\ell}, \tag{8}$$

where the first term corresponds to the interaction between the Li^{+q} and the outer electrons, and the second term is the addition over the different target bound shells. In the present contribution the stopping due to outer and inner electrons of Zn is calculated independently. For the outer or valence electrons, we employ the EFSR-TCS for a gas of electrons with $r_s=2.02$, corresponding to three electrons per atom of Zn. This stems from the experimental plasmon energy of 17 eV [25] which indicates the contribution, on the average, of one electron from the $3d$ shell, together with the two electrons from the valence band. For the inner shells ($1s$ up to $3d^9$) the calculation is performed by using the SLPA. Both models are summarized in the following sections.

A. Extended Friedel sum rule–transport cross section

This approach contains three basic steps. First, the screening of the ion by valence electrons is analyzed using quan-

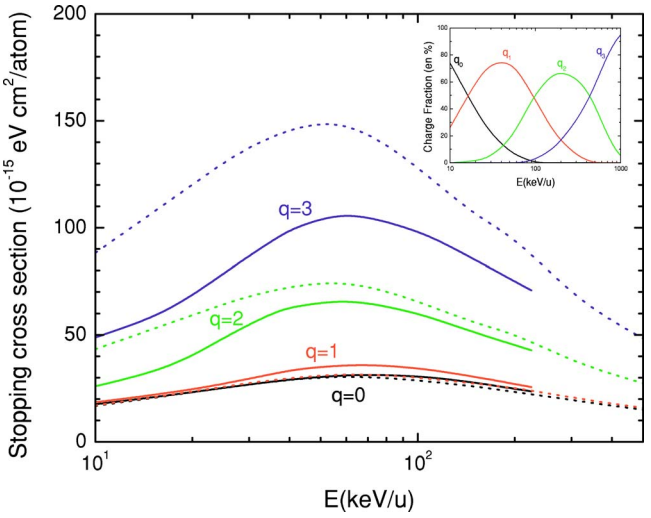

FIG. 3. (Color online) Valence electron contribution to the stopping cross section of Li^{+q} on Zn. The curves correspond to $q=0,1,2,3$ from down to top. Solid lines, nonperturbative EFSR-TCS calculations [7]; dotted lines, perturbative results using Mermin dielectric function [26]. Inset: Percentage of each charge state of Li ions in Zn as a function of the impact energy, given by the fitting to the experimental data outside the solid by Schiwietz and Grande [27].

tum scattering theory, starting with the calculation of the scattering phase shifts by direct numerical integration of the Schrödinger equation, and followed by an adjustment of the screening potential using the condition of overall neutralization of the ion charge by the surrounding medium as expressed by the extended Friedel sum rule, which applies to the case of moving ions [5]. Once the self-consistency is achieved, the transport cross section is evaluated, as a function of the relative electron-ion velocity. And finally, a complete integration over all possible relative velocities is performed (considering a moving ion with velocity v and a Fermi-Dirac type of distribution for the velocities of valence electrons in the target) [6,7]. This procedure is repeated for each ion charge state q and produces a partial stopping curve for each case. This approach may also be referred to as a nonlinear (or nonperturbative) calculation, needed at low impact energies, by distinction from the dielectric function method, which is perturbative and valid at high energies.

In Fig. 3 we display the EFSR-TCS results for the different charge states of the Li ions. These results are compared with those obtained by employing the dielectric formalism with the Mermin dielectric function [26], which is valid within the perturbative limits. The equilibrium charge states of Li in Zn depends on the impact velocity. The results of Schiwietz and Grande [27] are displayed in this figure as an inset.

The differences between the EFSR-TCS results and the dielectric calculations displayed in Fig. 3 are very important for Li^{+3} and Li^{+2} in Zn, showing the importance of nonlinear effects on a wide range of energies. On the contrary, for Li^0 and Li^+ the results of both descriptions are quite similar, indicating an almost perturbative behavior. We can also observe in this figure that while for Li^0 and Li^+ the nonperturbative results lie over the perturbative ones, the opposite occurs for higher charge values. This effect was commented upon in Ref. [7]. In general, the nonlinear stopping is enhanced over the linear one for low-charge projectiles [28], but with increasing ion charge, the nonlinear values increase with a lower rate than the linear ones. This is called "saturation effect" [7], and is a typical nonperturbative effect in the energy loss.

B. Shellwise local plasma approximation

The contribution to the stopping power of target bound electrons is calculated by employing the dielectric formalism for an inhomogeneous free electron gas. This method currently known as the local plasma approximation (LPA) was introduced by Lindhard and Scharff [8], and further developed by Bonderup [9], Chu and Powers [10], among others. A critical review of this method was presented by Johnson and Inokuti [11]. The current formulation is based on the dielectric formalism as proposed in previous papers [14], and mentioned as SLPA to emphasize the shell-to-shell calculation.

For an ion with charge state q and velocity v, the stopping cross section due to the ionization of the nl shell of target electrons, is expressed as

$$S_q^{nl} = \frac{2}{\pi v^2}\int_0^\infty \frac{dk}{k}\rho_q(k)\int_0^{kv}\omega\,\mathrm{Im}\left(\frac{-1}{\varepsilon^{nl}(k,\omega)}\right)d\omega, \qquad (9)$$

where $\rho_q(k)$ is given by Eq. (5). The dielectric function $\varepsilon^{nl}(k,\omega)$ is calculated as a mean value of a local response [29]

$$\mathrm{Im}\left(\frac{-1}{\varepsilon^{nl}(k,\omega)}\right) = 4\pi\int_0^{R_{\mathrm{WS}}}\mathrm{Im}\left(\frac{-1}{\varepsilon\left(k,\omega,k_{nl}^F(r)\right)}\right)r^2dr, \qquad (10)$$

where R_{WS} is the atomic Wigner-Seitz radius and $k_{nl}^F(r) = [3\pi^2\delta_{nl}(r)]^{1/3}$ is the local Fermi velocity. The spatial-dependent densities $\delta_{nl}(r)$ of each nl shell of Zn are obtained by employing the atomic Hartree-Fock wave functions [10].

The dielectric response, given by Eq. (10), considers only the electrons in the nl shell. In this way the contribution of each shell of target electrons is obtained separately. The orbital employment of the LPA was introduced by Meltzer *et al.* [30] in the logarithmic high-energy limit of the stopping number. In the SLPA, instead, we calculate a dielectric response of each shell, and it is valid even in the intermediate energy range. This model has already been employed successfully in the calculation of different moments of the energy, such as stopping power [14,31], energy loss straggling [32], and ionization cross sections [33] with good agreement with experimental data.

In the present version of the SLPA, we make an advance in the independent shell description by taking into account explicitly the energy threshold ϵ_{nl} of each shell. To this end, the Levine-Louie dielectric function [15] is employed instead of the Lindhard one [34]. The Levine and Louie model, proposed originally for semiconductors and insulators, defines the dielectric function as

$$\mathrm{Im}[\varepsilon^{\mathrm{LL}}(q,\omega,k_{nl}^F)] = \begin{cases} \mathrm{Im}[\varepsilon^L(q,\omega_g,k_{nl}^F)] & \omega > |\epsilon_{nl}|, \\ 0 & \omega < |\epsilon_{nl}|, \end{cases} \tag{11}$$

with $\omega_g = \sqrt{\omega^2 + \epsilon_{nl}^2}$ and $\varepsilon^L(q,\omega,k_{nl}^F)$ being the usual Lindhard dielectric function [34]. We want to remark that $\varepsilon^{\mathrm{LL}}$ satisfies the f-sum rule (particle number conservation). This modified SLPA has already been applied successfully in recent calculations of stopping power in insulators [35], but also in atomic collision calculations such as multiple ionization cross sections of rare gases [36].

V. RESULTS

In Fig. 2 we present our experimental and theoretical results for stopping cross sections of Li in Zn. In the region of overlap with previous data [3,4], at lower and higher energies, the agreement among the experimental values is quite good. We also include in the figure the semiempirical results by the SRIM 2006 code [1]. In the same figure we display the separate contributions of valence electrons by employing the EFSR-TCS, and inner-shell electrons using the SLPA. Our calculations are developed for the different charge states, but the total value is calculated by Eq. (3) weighting them with the empirical charge fraction distribution measured outside the solid [27]. We display theoretical results for electronic stopping within the interval 10 keV/u–10 MeV/u. Total results describe reasonably well the measurements for energies above 40 keV/u, with the largest difference being 8% around the stopping maximum, which is shifted in energies from 320 keV/u (experimental) to 520 keV/u (theoretical).

The employment of an inhomogeneous effective charge, given by Eq. (5), allows us to analyze the importance of the screening of the ion by its bound electrons. The screening effect is very important in stopping of heavy ions by the valence electrons, i.e., the stopping maximum decays from 1.06×10^{-13} eV cm^2/atom for Li^{+3} to 3.15×10^{-14} eV cm^2/atom for Li^0, as shown in Fig. 3. Instead, inner-shell stopping do not depend so critically on the screening (neutral and bare ion stopping differs less than 20% for energies below the stopping maximum).

In Fig. 4 we plot together the stopping of Zn for H, He, and Li ions, showing experimental data and our theoretical results. The general behavior of the stopping data is correctly described for the three ions, the maximum values appear shifted and moved down with respect to the stopping by bare ions. Also, the low-energy crossing of He and Li data is fairly well described. The difference between the calculation for bare ions, displayed as dotted lines in Fig. 4, and the measured stopping can only be explained taking into account the screening by the ion bound electrons, and its importance at each impact velocity (i.e., for energies below 100 keV most of the Li ions are Li^0 or Li^+).

VI. CONCLUDING REMARKS

In this work we present measurements of the stopping power for Li in Zn in the 300–5000 keV energy range using the RBS technique. By covering this energy range we were able to establish the behavior of the stopping power around its maximum which represents a real challenge for any theoretical description. The experimental results are in quite good agreement with previous experiments performed in a much narrower energy range and with the semiempirical predictions obtained from the SRIM 2006 algorithm.

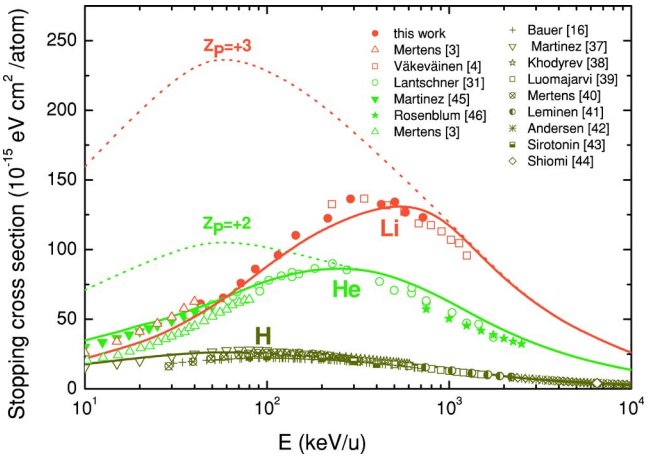

FIG. 4. (Color online) Total stopping of Zn for H, He, and Li ions. Symbols: experimental data for H [16,37–44], He [3,31,45,46], and Li [3,4]. Curves present theoretical calculations; solid lines, total results; dotted lines, results for bare ions.

On the other hand, we have performed first principle calculations taking into account the screening by the ion bound electrons in the different charge states. A nonperturbative formalism, the EFSR-TCS, is employed to calculate the valence electron contribution, which is the main one at low energies. A dielectric formalism for an inhomogeneous free electron gas, the SLPA, is employed for the target inner shells, which is the main contribution at high energies. Besides the fact that the calculated stopping maximum is shifted in energy, the description of the stopping cross section in the energy range 40 keV–10 MeV is reasonably good, with the largest difference of 8% around the stopping maximum. The comparison of the stopping curves for H, He, and Li ions shows that the model works well in all these cases, emphasizing the importance of the screened picture and nonlinear effects, especially for the interaction with the valence electrons.

ACKNOWLEDGMENTS

This work was partially supported by the Universidad de Buenos Aires (UBACyT X870 and X259), the Agencia Nacional de Promoción Científica y Tecnológica of Argentina (PICT R122/02 and PICT R437/03), the Consejo Nacional de Investigaciones Científicas y Técnicas (CONICET, PIP 6268), and the CNPQ from Brazil. The participation of Esteban Cantero in the final version of the paper is gratefully acknowledged.

[1] J. F. Ziegler and J. P. Biersack, SRIM2006—The stopping and range of ions in matter, Version 2006, code available in http://www.srim.org
[2] H. Paul, Stopping power for light ions. Graphs, data, comments and programs, http://www.exphys.uni-linz.ac.at/stopping/
[3] P. Mertens and Th. Krist, J. Appl. Phys. **53**, 7343 (1982).
[4] K. Väkeväinen, Nucl. Instrum. Methods Phys. Res. B **122**, 187 (1997).
[5] A. F. Lifschitz and N. R. Arista, Phys. Rev. A **57**, 200 (1998).
[6] A. F. Lifschitz and N. R. Arista, Phys. Rev. A **58**, 2168 (1998).
[7] N. R. Arista, Nucl. Instrum. Methods Phys. Res. B **195**, 91 (2002).
[8] J. Lindhard and M. Scharff, K. Dan. Vidensk. Selsk. Mat. Fys. Medd. **27**, 15 (1953).
[9] E. Bonderup, K. Dan. Vidensk. Selsk. Mat. Fys. Medd. **35**, 17 (1967).
[10] W. K. Chu and D. Powers, Phys. Lett. **40A**, 23 (1972).
[11] R. E. Johnson and M. Inokuti, Comments At. Mol. Phys. **14**, 19 (1983).
[12] C. J. Tung, R. L. Shyu, and C. M. Kwei, J. Phys. D **21**, 1125 (1988).
[13] A. Sarasola, J. D. Fuhr, V. H. Ponce, and A. Arnau, Nucl. Instrum. Methods Phys. Res. B **182**, 67 (2001).
[14] C. C. Montanari and J. E. Miraglia, Phys. Rev. A **73**, 024901 (2006).
[15] Z. H. Levine and S. G. Louie, Phys. Rev. B **25**, 6310 (1982).
[16] P. Bauer, F. Kastner, A. Arnau, A. Salin, P. D. Fainstein, V. H. Ponce, and P. M. Echenique, Phys. Rev. Lett. **69**, 1137 (1992).
[17] H. H. Andersen and J. F. Ziegler, "Hydrogen stopping powers and ranges in all elements," in *Stopping and Ranges of Ions in Matter*, edited by J. F. Ziegler (Pergamon, New York, 1977), Vol. 3.
[18] N. Bohr, K. Dan. Vidensk. Selsk. Mat. Fys. Medd. **18**, 8 (1948).
[19] W. K. Chu, J. W. Mayer, and M. A. Nicolet, *Backscattering Spectrometry* (Academic, New York, 1978).
[20] P. Sigmund, *Particle Penetration and Radiation Effects* (Springer, New York, 2006).
[21] A. Dalgarno and G. W. Griffing, Proc. R. Soc. London, Ser. A **232**, 423 (1955).
[22] E. C. Montenegro and W. E. Meyerhof, Phys. Rev. A **43**, 2289 (1991).
[23] C. Reinhold and J. E. Miraglia, J. Phys. B **20**, 1069 (1987).
[24] E. Clementi and C. Roetti, At. Data Nucl. Data Tables **14**, 177 (1974).
[25] D. Isaacson, New York University Report No. 02698 (National Auxiliary Publication Service, New York, 1975).
[26] N. D. Mermin, Phys. Rev. B **1**, 2362 (1970).
[27] G. Schiwietz and P. L. Grande, Nucl. Instrum. Methods Phys. Res. B **175–177**, 125 (2001); CasP version 3.1, code available at www.hmi.de/people/schiwietz/casp.html
[28] A. Mann and W. Brandt, Phys. Rev. B **24**, 4999 (1981).
[29] J. D. Fuhr, V. H. Ponce, F. J. García de Abajo, and P. M. Echenique, Phys. Rev. B **57**, 9329 (1998).
[30] D. E. Meltzer, J. R. Sabin, and S. B. Trickey, Phys. Rev. A **41**, 220 (1990).
[31] G. H. Lantschner, J. C. Eckardt, A. F. Lifschitz, N. R. Arista, L. L. Araujo, P. F. Duarte, J. H. R. dos Santos, M. Behar, J. F. Dias, P. L. Grande, C. C. Montanari, and J. E. Miraglia, Phys. Rev. A **69**, 062903 (2004).
[32] C. C. Montanari, J. E. Miraglia, S. Heredia-Avalos, R. Garcia-Molina, and I. Abril, Phys. Rev. A **75**, 022903 (2007).
[33] U. Kadhane, C. C. Montanari, and L. C. Tribedi, Phys. Rev. A **67**, 032703 (2003); J. Phys. B **36**, 3043 (2003).
[34] J. Lindhard, K. Dan. Vidensk. Selsk. Mat. Fys. Medd. **28**, 8 (1954).
[35] A. J. Garcia and J. E. Miraglia, Phys. Rev. A **74**, 012902 (2006).
[36] C. D. Archubi, C. C. Montanari, and J. E. Miraglia, J. Phys. B **40**, 943 (2007).
[37] G. Martinez-Tamayo, J. C. Eckardt, G. H. Lantschner, and N. R. Arista, Phys. Rev. A **51**, 2285 (1995).
[38] V. A. Khodyrev, V. N. Mizgulin, E. I. Sirotonin, and A. F. Tulinov, Radiat. Eff. **83**, 21 (1984).
[39] M. Luomajärvi, Radiat. Eff. **40**, 173 (1979).
[40] P. Mertens and Th. Krist, Nucl. Instrum. Methods Phys. Res. **194**, 57 (1982).
[41] E. Leminen, A. Fontell, and M. Bister, Ann. Acad. Sci. Fenn., Ser. A VI Phys. **6**, 281 (1968).
[42] H. H. Andersen, C. C. Hanke, H. Simonsen, H. Sörensen, and P. Vajda, Phys. Rev. **175**, 389 (1968).
[43] E. I. Sirotinin, A. F. Tulinov, V. A. Khodyrev, and V. N. Mizgulin, Nucl. Instrum. Methods Phys. Res. B **4**, 337 (1984).
[44] N. Shiomi-Tsuda, N. Sakamoto, and R. Ishiwari, Nucl. Instrum. Methods Phys. Res. B **93**, 391 (1994).
[45] G. Martinez-Tamayo, J. C. Eckardt, G. H. Lantschner, and N. R. Arista, Phys. Rev. A **54**, 3131 (1996).
[46] S. Rosenblum, Ann. Phys. **10**, 408 (1928).